

# Prevention of acute graft-vs.-host disease by targeting glycolysis and mTOR pathways in activated T cells

RUI-QING ZHOU<sup>1\*</sup>, XIAOBO WANG<sup>2\*</sup>, YONG-BIN YE<sup>3\*</sup>, BO LU<sup>2</sup>, JING WANG<sup>4</sup>, ZI-WEN GUO<sup>3</sup>, WEN-JIAN MO<sup>1</sup>, ZHENG YANG<sup>5</sup>, PATHOMTHAT SRISUK<sup>6</sup>, LE-PING YAN<sup>2,7</sup> and XIAO-JUN XU<sup>2,3</sup>

<sup>1</sup>Department of Hematology, Guangzhou First People's Hospital, The Second Affiliated Hospital of South China University of Technology, Guangzhou, Guangdong 510180; <sup>2</sup>Department of Hematology, The Seventh Affiliated Hospital, Sun Yat-sen University, Shenzhen, Guangdong 518107; <sup>3</sup>Department of Hematology, Zhongshan Hospital of Sun Yat-Sen University and Zhongshan City People's Hospital, Zhongshan, Guangdong 528403; <sup>4</sup>Nanfang-Chunfu Children's Institute of Hematology and Oncology, TaiXin Hospital, Dongguan, Guangdong 523128; <sup>5</sup>Department of Pathology, The Seventh Affiliated Hospital, Sun Yat-sen University, Shenzhen, Guangdong 518107, P.R. China; <sup>6</sup>Division of Pharmaceutical Technology, Faculty of Pharmaceutical Sciences, Khon Kaen University, Khon Kaen 40002, Thailand; <sup>7</sup>Scientific Research Center, The Seventh Affiliated Hospital, Sun Yat-sen University, Shenzhen, Guangdong 518107, P.R. China

Received August 8, 2021; Accepted February 18, 2022

DOI: 10.3892/etm.2022.11375

**Abstract.** Graft-versus-host disease (GvHD) is a common life-threatening complication that can occur following allogeneic hematopoietic stem cell transplantation. This occurs if donor T cells recognize the host as foreign. During acute GvHD (aGVHD), activated T cells utilize glycolysis as the main source of energy generation. Therefore, inhibition of T cell glycolysis is a potential treatment strategy for aGVHD. In the present study, the effects of the combination of the glycolysis inhibitor 3-bromopyruvate (3-BrPA) and the mTOR inhibitor rapamycin (RAPA) on a mode of aGVHD were explored. *In vitro* mixed lymphocyte culture model was established by using splenocytes from C57BL/6 (H-2b) mice as responder and inactivated splenocytes from BALB/c (H-2d) mice as stimulator. In this model, 3-BrPA treatment (0-100  $\mu$ mol/l) was found to suppress cell viability, increase cell apoptosis and reduce IFN- $\gamma$  secretion, in a concentration-dependent manner.

3-BrPA treatment (0-100  $\mu$ mol/l) was found to suppress cell viability, increase cell apoptosis and reduce IFN- $\gamma$  secretion, in a concentration-dependent manner. In addition, combined treatment with 3-BrPA (0-100  $\mu$ mol/l) alongside RAPA (20  $\mu$ mol/l) exhibited synergistic effects on inhibiting cell viability and IFN- $\gamma$  production, compared with those following either treatment alone. An aGVHD model was established by injection of bone marrow cells and spleen cells from the donor-C57BL/6(H-2b) mice to the receptor-BALB/c(H-2d) mice which were underwent total body irradiation first. In the aGVHD model, 3-BrPA (10 mg/kg/day), RAPA (2.5 and 5 mg/kg/day) and both in combination (5 and 2.5 mg/kg/day for 3-BrPA and RAPA, respectively) were all found to alleviate the damage caused by aGVHD, in addition to prolonging the survival time of mice with acute GvHD. In particular, the combined 3-BrPA and RAPA treatment resulted in the highest median survival time among all groups tested. In addition, the effects induced by combined 3-BrPA and RAPA treatment were found to be comparable to those in the 5 mg/kg/day RAPA group but superior to the 3-BrPA group with regards to the cumulative survival profile, GvHD score and lung histological score. The 3-BrPA and RAPA combination group also exhibited the lowest IFN- $\gamma$  levels among all groups. Therefore, the combination of inhibiting both glycolysis and mTOR activity is a promising strategy for acute GvHD prevention.

*Correspondence to:* Professor Le-Ping Yan, Scientific Research Center, The Seventh Affiliated Hospital, Sun Yat-sen University, 628 Zhenyuan Road, Shenzhen, Guangdong 518107, P.R. China  
E-mail: yanlp3@mail.sysu.edu.cn

Professor Xiao-Jun Xu, Department of Hematology, The Seventh Affiliated Hospital, Sun Yat-sen University, 628 Zhenyuan Road, Shenzhen, Guangdong 518107, P.R. China  
E-mail: xuxj29@mail.sysu.edu.cn

\*Contributed equally

**Key words:** hematopoietic stem cell transplantation, glycolysis inhibition, rapamycin, 3-bromopyruvate, acute graft versus host disease, mixed lymphocytes culture

## Introduction

Hematopoietic stem cell transplantation (HSCT) is an important treatment method for a number of refractory malignant hematopoietic disorders, such as myelodysplastic syndrome, T-cell lymphomas, multiple myeloma, and chronic myelomonocytic leukemia (1-4). However, successful applications of HSCT are frequently limited by relapse and graft-versus-host disease (GvHD) (5,6). The pathogenesis of acute GvHD

(aGVHD) is associated with the activation of donor T cells (5). Therefore, effective inhibition of activated T cells (effector T cells) in the donor sample is key for the prophylaxis and treatment of aGVHD (5).

Activated T cells require a constant source of energy production to meet the demands caused by rapid proliferation (7). Aerobic glycolysis has been previously recognized to be the main metabolic pathway activated in effector T cells during GVHD (8-11). However, fatty acid oxidative phosphorylation has also been reported to be active in activated T cells (8-11). Similar to activated T cells, cancer cells also depend on glycolysis for ATP generation, such that glycolysis inhibition has demonstrated efficacy in the inhibition of leukemia, lymphoma and testicular tumor cells (12-14). In a previous study by Nguyen *et al.* (8), it was shown that allo-antigen-activated T cells required glycolysis for optimal function in a murine bone marrow transplant model. Therefore, inhibition of glycolysis can be a feasible intervention option for aGVHD prevention.

The compound of 3-bromopyruvate (3-BrPA) is an effective glycolysis inhibitor that can target both hypoxia-inducible factor (HIF)-1 $\alpha$  and GAPDH pathways (15-17). It has also been reported to exert anti-cancer effects by inhibiting aerobic glycolysis in cancer cells, such as breast and colorectal cancer cells (17). In addition, it has been demonstrated to reverse resistance to anti-cancer drugs by suppressing the activity of the ATP-dependent multi-drug resistance transporter (17). However, inhibition of glycolysis and the subsequently reduced glucose metabolic activity/ATP concentration will activate the mTOR pathway, producing compensatory survival signals (12).

Rapamycin (RAPA) was the first mTOR inhibitor to be generated and has been applied for the treatment of various types of malignancies, including breast, leukemia, prostate, lung and skin (18). It has also been used as an immunosuppressor for GVHD prevention (7). A previous study has revealed that RAPA treatment can induce the accumulation of regulatory T cells (Treg) in the skin of mice after bone marrow transplantation (19). In a recent study, Scheurer *et al.* (20) found that RAPA treatment can increase the immunosuppressive potential of myeloid-derived suppressor cells (MDSCs) whilst maintaining the anti-tumor cytotoxicity of T cells [Graft vs. tumor (GvT)] without impairing the induction of Treg in a bone marrow transplantation mouse model (20). However, other *in vitro* studies and clinical findings demonstrated that the development of RAPA resistance typically occurs (21). In addition, toxicity is another concern of this drug (8). Therefore, combination of low doses of RAPA with glycolysis inhibitors may serve to be an attractive treatment option, since it may maintain the efficacy of these drugs for the suppression of GVHD whilst preventing the resistance and toxicity effects of RAPA.

The effects of combined treatment with RAPA and 3-BrPA for aGVHD remain poorly understood. Therefore, in present study, the efficacy of combined 3-BrPA and RAPA treatment on the pathogenesis of aGVHD, on glycolysis and mTOR signaling in activated T cells was investigated.

## Materials and methods

**Animals.** A total of 94 male C57BL/6 (H-2b) mice (age, 8 weeks; weight, 18.7 $\pm$ 0.7 g) and 21 female BALB/c (H-2d)

mice (age, 8 weeks; weight, 19.0 $\pm$ 0.5 g) were obtained from Southern Medical University (Guangzhou, China). All mouse studies were approved by the Ethics Committee of Southern Medical University, performed in The Experimental Animal Center of Southern Medical University and fulfilled the regulations of The Institutional Animal Care and Use Committee (IACUC). In total, four mice were housed in a cage with free access to food pellets and drinking water. The mice were maintained in conditions of 21 $\pm$ 2°C, relative humidity of 40-60% and a 12-h light-dark cycle.

**Isolation of splenocytes.** In total, three female BALB/c (H-2d) mice and three male C57BL/6 (H-2b) mice were used for the isolation of splenocytes by following a previously reported protocol (22). Briefly, the mice were sacrificed by cervical dislocation before the spleen was collected. Subsequently, the spleen was cut into small pieces by using an ophthalmic scissors and then ground with the plunger handle of a syringe on a plastic plate in a sterile biosafety cabinet at room temperature to release the splenocytes. The cells were collected in a centrifuge tube after washing with PBS and then lysed with red blood cell lysis buffer (Beyotime Institute of Biotechnology). The lysis was performed followed the manufacturer's instruction. Briefly, the cells were mixed with the lysis working solution at room temperature for 2 min with gentle shaking. Afterwards, the cells were collected by centrifuge at 400 g for 5 min at 4°C. This step was repeated until cracking was completed. The isolated splenocytes were cultured with RPMI-1640 medium (Thermo Fisher Scientific, Waltham, MA, USA) supplemented with 10% fetal bovine serum (FBS, Beyotime Institute of Biotechnology) in an incubator under 37°C and 5% CO<sub>2</sub>.

**RAPA- and 3-BrPA-supplemented one-way mixed lymphocyte reaction (MLR).** Splenocytes isolated from the male C57BL/6 (H-2b) mice as designated to be responders, whereas splenocytes isolated from the female BALB/c (H-2d) mice were inactivated by mitomycin-C (MilliporeSigma) at room temperature for 2 h (10  $\mu$ g/ml) before being designated to be stimulators. A total of 5 $\times$ 10<sup>5</sup> responder cells (0.1 ml) and an equivalent density of stimulator cells (0.1 ml) were co-cultured in the 96-well cell culture plate supplemented with RPMI 1640 medium (Thermo Fisher Scientific, Waltham, MA, USA), supplemented with 10% FBS (Beyotime Institute of Biotechnology), 1% Penicillin-streptomycin (MilliporeSigma) and 1% 1% glutamine (MilliporeSigma). RAPA, 3-BrPA or the combination of both RAPA and 3-BrPA, at concentrations ranging from 0-100  $\mu$ M, were added into the mixed lymphocyte culture (MLC). RAPA and 3-BrPA were obtained from MilliporeSigma. The RAPA and 3-BrPA stock solutions were prepared by dissolving in DMSO to produce 10 mmol/l and stored at -20°C before use. For cell culture, quantities of RAPA and 3-BrPA stock solutions were added into the medium at room temperature to achieve the required final concentrations. An equivalent amount of DMSO was added as the control. These cells were maintained in an incubator under standard cell culture conditions of 37°C, 90% humidity and 5% CO<sub>2</sub>. The cells were analyzed after 24 and 48 h of culture.

**Glucose consumption, cellular viability and synergistic effect evaluations.** Glucose consumption of cells in the MLC

was evaluated using the Glucose (HK) Assay kit (GAHK20, MilliporeSigma) according to the manufacturer's protocol to test the efficiency of glycolysis inhibition. Cells without any drug treatment was used as control. This glucose consumption assay is used to measure the conversion of glucose into 6-phosphogluconate and reduced NADH to reflect the activity of glycolysis.

The viability of the cells in the MLC was measured 24 and 48 h after culture by using the Cell Counting Kit-8 (CCK-8; Dojindo Molecular Technologies, Inc.) according to the manufacturer's protocol. Briefly, 20  $\mu$ l CCK-8 was added into each well and incubated under 37°C, 5% CO<sub>2</sub> and 100% humidity in a cell incubator for 2 h. The absorbance of the cell culture medium was measured at 450 nm wavelength in a microplate reader (Wallac 1420 Victor2, Perkin Elmer).

The degree of synergism between 3-BrPA and RAPA was calculated using the Chou-Talalay method (23). For any inhibition ratios exerted by the combination treatment of 3-BrPA and RAPA according to the cell viability data, if the combination index (CI) was calculated to be <1, this would be considered that this particular combination of combined treatment in question exhibits a synergistic effect.

**Cell apoptosis evaluation.** The MLC were harvested after culture for 48 h and washed once by PBS before the staining. Cells were centrifuge at 400 x g for 5 min, and subsequently resuspended in Annexin V binding buffer (Cell Apoptosis Analysis Kit, KGA108, Nanjing KeyGen Biotech Co., Ltd). For the staining, 5  $\mu$ l FITC-Annexin V and 10  $\mu$ l propidium iodide solutions were added into 100  $\mu$ l cell suspension (1x10<sup>5</sup> cells in binding buffer) and the cells were stained for 15 min at room temperature according to the manufacturer's protocol. After the staining, the cells were analyzed by flow cytometry (CytoFLEX, Beckman Coulter, Brea, CA, USA). The flow cytometric data were analyzed by using the FlowJo V10 software (BD Life Sciences-FlowJo).

**ELISA.** The supernatant of the MLC was collected after treatment with 3-BrPA and/or RAPA for 48 h. The concentrations of IL-4 and IFN- $\gamma$  in the supernatant were then measured by using the mouse IL-4 ELISA kit (Cat: P1612) and mouse IFN- $\gamma$  ELISA kit (Cat: 1508) according to the manufacturer's protocols (Beyotime Institute of Biotechnology). The IL-4 and IFN- $\gamma$  levels in the serum of mice with aGVHD were also measured by ELISA 7 days after transplantation, using the same products and protocol.

**Establishment of the aGVHD model and drug administration.** The aGVHD model was established by the injection of bone marrow cells and spleen cells from the donor male C57BL/6 (H-2b) mice, which were sacrificed by cervical dislocation, to the receiver female BALB/c (H-2d) mice (24,25). In total, 91 female receiver BALB/c (H-2d) mice and 16 male donor C57BL/6 (H-2b) mice were used for the aGVHD study. The C57BL/6(H-2b) mice was used for extraction of the splenocytes and bone marrow cells for transplantation into the BALB/c (H-2d) mice, and cells isolated from 16 C57BL/6 (H-2b) mouse were used for transplantation into 78 BALB/c (H-2d) mice (1 to 5). The study groups were designated as follows (n=13): i) TBI group, where the receiver mice only underwent TBI;

ii) aGVHD group, which is identical with the TBI group except for being transplanted with both bone marrow and spleen cells after TBI; iii) RAPA-2.5 mg group, which is identical to the aGVHD group but was treated with RAPA (2.5 mg/kg/day) for 7 days; iv) RAPA-5 mg group, which is the aGVHD group treated with RAPA (5 mg/kg/day) for 7 days; v) 3-BrPA group, which is the aGVHD group treated with 3-BrPA (10 mg/kg/day) for 7 days; vi) combination group, which is the aGVHD group treated with both RAPA (2.5 mg/kg/day) and 3-BrPA (5 mg/kg/day) for 7 days; and vii) bone marrow transplantation (BMT) group, which was the TBI group that was only transplanted with bone marrow cells (6x10<sup>5</sup>).

The isolation of splenocytes was performed as aforementioned. For isolation of bone marrow cells, the femurs of the mice were first separated from the hind legs, and the bone marrow plug was subsequently flushed out by using PBS after the epiphyseal head were removed. The cells were filtrated using 70  $\mu$ l nylon mesh after pipetting in the 15 ml plastic centrifuge tube. The cells were lysed with red blood cell lysis buffer (Beyotime Institute of Biotechnology) using protocol as mentioned above. The isolated bone marrow cells and splenocytes were suspended in RPMI-1640 medium (Thermo Fisher Scientific, Inc.) supplemented with 10% fetal bovine serum (FBS, Beyotime Institute of Biotechnology) in an incubator under 37°C and 5% CO<sub>2</sub> before transplantation. These cells were transplanted within 3 h after preparation.

The total body irradiation (TBI) was performed to kill the hemopoietic stem cells of the recipient mice. Each recipient mice received total 8 Gy (0.5 Gy/min, room temperature) TBI X-ray irradiation (Varian 2100C/D, Varian Medical Systems, Palo Alto, CA, USA). For the transplantation, 6x10<sup>5</sup> bone marrow cells and/or 6x10<sup>5</sup> splenocytes from donor mice were transplanted into each receiver mouse by tail vein injection  $\leq$ 4 h after 7.5 Gy total body irradiation (TBI) performed for 15 min at room temperature. Various drugs were then intraperitoneal injection to each mouse 1 h after the injection of cells. For animal experiments, the RAPA and 3-BrPA stock solutions were diluted using 1X PBS for intraperitoneal injection into the mice (20). The aGVHD and BMT groups were injected with an equivalent amount of DMSO but without drugs.

**Chimeric rate examination.** To determine the chimeric rate in the transplanted mice, the mice were first anesthetized by injection with pentobarbital sodium (50 mg/kg) 11 days (4 days without further treatment) after transplantation, before ~2 mm of the tail was cut and 50  $\mu$ l blood was collected from the tail vein of each mouse using a micropipette. The blood was diluted by addition of 150  $\mu$ l EDTA solution. MHC Class I (H-2Kb) Monoclonal Antibody (AF6-88.5.5.3), FITC (eBioscience, Thermo Fisher Scientific, Waltham, MA, USA) were added into the diluted blood and incubated for 20 min at room temperature. Then, the cells were assessed by a flow cytometer (BD FACSCANTO II, BD Biosciences). The flow cytometer detected the FITC-positive cells, and the ratio of these positive cells in each tested aliquot was analyzed by using FlowJo V10 software (BD Life Sciences-FlowJo, Ashland, OR, USA) and defined as the allogeneic chimeric rate. The aGVHD, RAPA-2.5 mg, RAPA-5 mg, 3-BrPA, RAPA and 3-BrPA combination and BMT groups were analyzed by using cells from three mice/group.

**Survival analysis.** The cumulative survival curves of the mice in each group were calculated using the Kaplan-Meier method. For the calculation of median survival time and comparison of the survival results among the groups, log-rank test was performed followed by Bonferroni's correction was applied.  $P < 0.00238$  was considered to indicate a statistically significant difference for the comparison of the seven groups in this case.

**GvHD scoring.** The GvHD scores of the mice were calculated by measurement of five parameters (weight loss, posture, activity, fur texture and skin integrity) as previously described by Cooke *et al* and the grade details were mentioned in Table I (26). In this evaluation system, the severity of GvHD was quantified by the change percentage of each parameter and graded from 0 (normal or reduced less than 10%), 1 (reduced 10-30%; mild reduced), and 2 (reduced >30% or serious change observed) for each criterion. The final GvHD score was obtained by summation of scores of the five criteria. None of the mice received any further treatment after 7 days. Scores were recorded on day 7, 14 and 21. No mouse survived in the aGVHD group 14 days after transplantation.

**Histological analysis.** Tissue response to aGVHD in the main organs of the mice, specifically the lung and liver, were assessed by H&E histological staining after euthanasia by cervical dislocation. The organs were harvested 12 days after transplantation (3 mice/group) and then fixed in 4% paraformaldehyde under room temperature for 24 h before paraffin embedding. The sections of 4  $\mu\text{m}$  thickness were obtained by using a rotary microtome (Leica RM2235, Leica Biosystems). The hematoxylin and Eosin (H&E) staining was conducted under room temperature. Briefly, the sections were firstly deparaffinized by in two changes of xylene (10 min each immersion), subsequently the sections were rehydrated by immersion in two changes of 100% alcohol with 5 min for each, and then in 95% alcohol for 5 min, in 70% alcohol for 5 min. After that, the slides were washed in distilled water and stained in hematoxylin for 1 min, followed by washing in tap water for 30 sec. Following, the slides were immersed in 1% acid alcohol superfast differentiation solution for 15 sec (Beyotime Institute of Biotechnology, Shanghai, China), followed by washing in tap water for 15 sec. Afterwards, the slides were counterstained in eosin solution for 15 sec. The slides were then dehydrated by immersion in a series of one 95% alcohol for 5 min, two changes of 100% alcohol with 5 min for each and two changes of xylene with 15 sec for each. Then, the slides were mounted with mounting medium. Images of the slides were taken at 20X magnification in a Leica DM6B upright fluorescence microscope (Leica Biosystems, Wetzlar, Germany). The staining images were then scored by three independent pathologists who were blinded before scoring, with normal as 1, slight tissue damage as 2, mild tissue damage as 3 and severe tissue damage as 4.

**Statistical analysis.** Results of cellular viability, cellular apoptosis, IL-4, IFN- $\gamma$  and the glucose consumption are presented as mean  $\pm$  standard deviation. Median scores were presented in GvHD scores and histological scores. GraphPad Prism (Version 8.0.2, GraphPad Software, Inc.) was used for data processing. In cases where there were two variables (RAPA

and 3-BrPA), two-way ANOVA followed by Sidak's post hoc test was performed. For the analysis of the Kaplan-Meier's survival results, log-rank test was performed followed by the Bonferroni's correction. In this case,  $P < 0.00238$  was considered to indicate a statistically significant difference for the comparison of the seven groups. The statistical analysis of the GvHD and histological scores results was conducted by using Kruskal-Wallis test followed by the Dunn's post hoc test. For the analysis of the *in vivo* IL-4 and IFN- $\gamma$  results, one-way ANOVA followed by Tukey's test was performed. All experiments were repeated twice except aGVHD mouse study was performed once) and  $\geq$  three samples were tested for each test at each timepoint. Apart from the Kaplan-Meier analysis,  $P < 0.05$  was considered to indicate a statistically significant difference.

## Results

**Cellular viability and synergistic effect evaluation.** It was found that the 3-BrPA treatment can effectively inhibit the glucose consumption in a dose-dependent manner (Fig. S1). For the 3-BrPA-alone treatment groups, increasing the 3-BrPA concentration from 10 to 100  $\mu\text{M}$  progressively decreased glucose consumption (Fig. S1). Significant glucose consumption inhibition effect were observed for RAPA-alone treatment compared to control (0  $\mu\text{M}$  3-BrPA). In the combination treatment groups, the addition of RAPA alongside 3-BrPA induced significant reductions in glucose consumption at each tested concentration of 3-BrPA (Fig. S1). Furthermore, increasing 3-BrPA concentration from 0 to 100  $\mu\text{M}$  induced significant reductions in glucose consumption in the combination groups in a dose-dependent manner (Fig. S1).

In terms of cell viability (Fig. 1), both 3-BrPA and combined treatment exerted significant effects on the inhibition of cell viability at both 24 and 48 h, where there were cumulative effect between 3-BrPA and RAPA on cell viability at both time points based on the two-way ANOVA analysis. After 24 h (Fig. 1A), there was no statistical significance in cell viability between the 0 and 10  $\mu\text{M}$  3-BrPA treatment-alone groups. However, treatment with 20, 50 and 100  $\mu\text{M}$  3-BrPA alone induced decreases in cell viability compared with that in the 0 or 10  $\mu\text{M}$  3-BrPA-alone groups (Fig. 1A). Additionally, the cellular viability decreased as 3-BrPA concentration increased from 20 to 100  $\mu\text{M}$  (Fig. 1A). RAPA co-treatment exerted significant reduction in cell viability at each 3-BrPA concentration compared with that in their corresponding 3-BrPA-alone counterparts (Fig. 1A). Among the combined treatment groups, the 0  $\mu\text{M}$  3-BrPA combination treatment group showed no significant differences compared with that in the 10  $\mu\text{M}$  3-BrPA combination treatment group. However, cell viability was significantly decreased in the combination treatment groups of 20, 50 and 100  $\mu\text{M}$  3-BrPA compared with that in the 0  $\mu\text{M}$  group (Fig. 1A). In addition, the cellular viability decreased remarkably when the 3-BrPA concentration increased from 20 to 100  $\mu\text{M}$  in the combination treatment groups (Fig. 1A).

After 48 h of treatment (Fig. 1B), the cellular viability reduced as increasing the 3-BrPA concentration from 0 to 100  $\mu\text{M}$  (Fig. 1B). Combined treatment with 3-BrPA and RAPA mediated significant reductions in cell viability

Table I. Graft vs. host disease scores in the transplanted mice.

Parameter	0	1	2
Weight loss	Reduced <10%	Reduced 10-25%	Reduced >25%
Posture	Normal	Hunching only at rest	Serious hunching
Activity	Normal	Mild to moderately reduced	No activity unless stimulated
Fur texture	Normal	Mild to Moderate ruffling	Serious ruffling
Skin integrity	Normal	Scaling of paws/tail	Significantly denuded skin

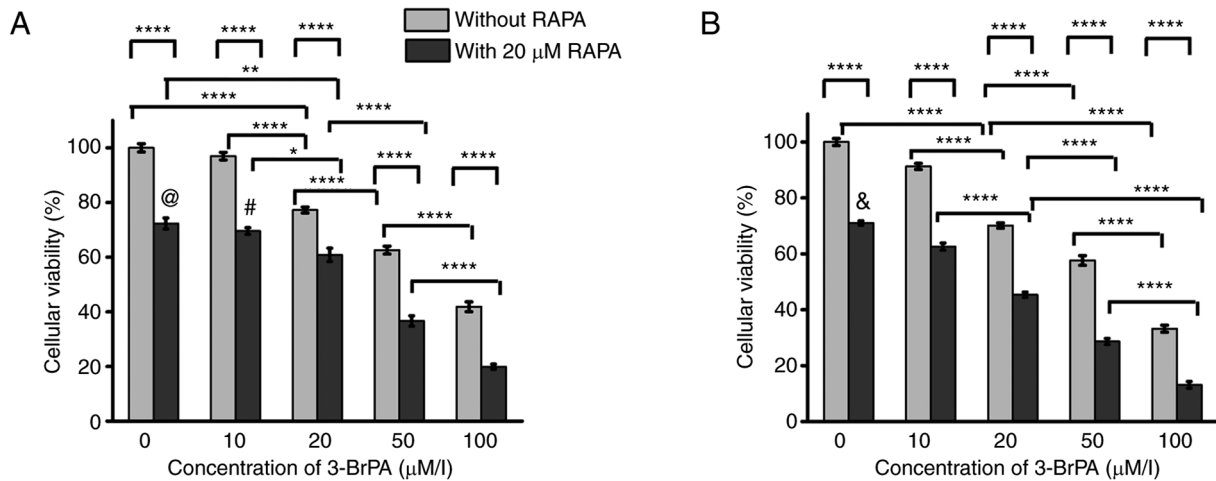


Figure 1. Cellular viability analysis of the MLC. Cellular viability analysis of the MLC after treatment of 3-BrPA and RAPA for (A) 24 and (B) 48 h. At each time point, cellular viability was determined using the Cell Counting Kit-8 method and was presented as percentage of the optical value in each group relative to that in the control group (no drug treatment, set as 100%). \*P<0.05, \*\*P<0.005, \*\*\*\*P<0.0001. In (A), @P<0.0001, #P<0.0001 compared to combination group with 50 μM 3-BrPA. In (B), &P<0.0001 compared to 10 μM 3-BrPA group. MLC, mixed lymphocyte culture; RAPA, rapamycin; 3-BrPA, 3-bromopyruvate.

compared with that in their corresponding 3-BrPA-alone groups at each 3-BrPA concentration tested (Fig. 1B). Among the combination treatment groups, the cellular viability also decreased when increasing the 3-BrPA concentration from 0 to 100 μM (Fig. 1B).

Subsequently, the CI of the combined treatment of 3-BrPA and RAPA were calculated. After the MLC has been treated with both 20 μM 3-BrPA and 20 μM RAPA for 24 h, the ~39% inhibition ratio corresponded to a CI value of 0.71. After 48 h of treatment, the 20 μM 3-BrPA and 20 μM RAPA combined treatment induced ~55% inhibition ratio, which corresponded to a CI value of 0.44.

**Cell apoptosis in the MLC.** As shown in Figs. 2 and S2, both 3-BrPA treatment alone and when combined with RAPA mediated significant inhibition effects on apoptosis. After treatment with 3-BrPA alone, significant increases in apoptosis were found after comparing the 0 μM 3-BrPA-alone group with the 20, 50 or 100 μM 3-BrPA treatment group (Figs. 2 and S2). Additionally, the cellular apoptosis improved as increasing the 3-BrPA concentration from 10 to 100 μM (Figs. 2 and S2). After the cells were treated with the combination of 3-BrPA and RAPA, apoptosis was significantly increased compared with that in their corresponding 3-BrPA-alone groups at each concentration tested (Figs. 2 and S2). Among the combination treatment groups, there were significant enhancement in cellular apoptosis by comparing the 0 μM to the 20, 50 μM or

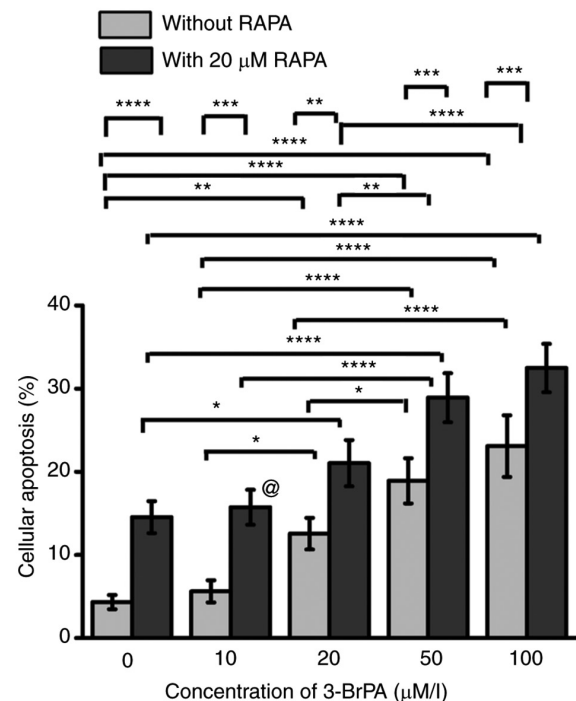


Figure 2. Cell apoptosis evaluation of the MLC by flow cytometry after combined treatment with 3-BrPA and RAPA for 48 h. \*P<0.05, \*\*P<0.005, \*\*\*P<0.001, \*\*\*\*P<0.0001. @P<0.0001 compared to the combination treatment group with 100 μM 3-BrPA. MLC, mixed lymphocyte culture; RAPA, rapamycin; 3-BrPA, 3-bromopyruvate.

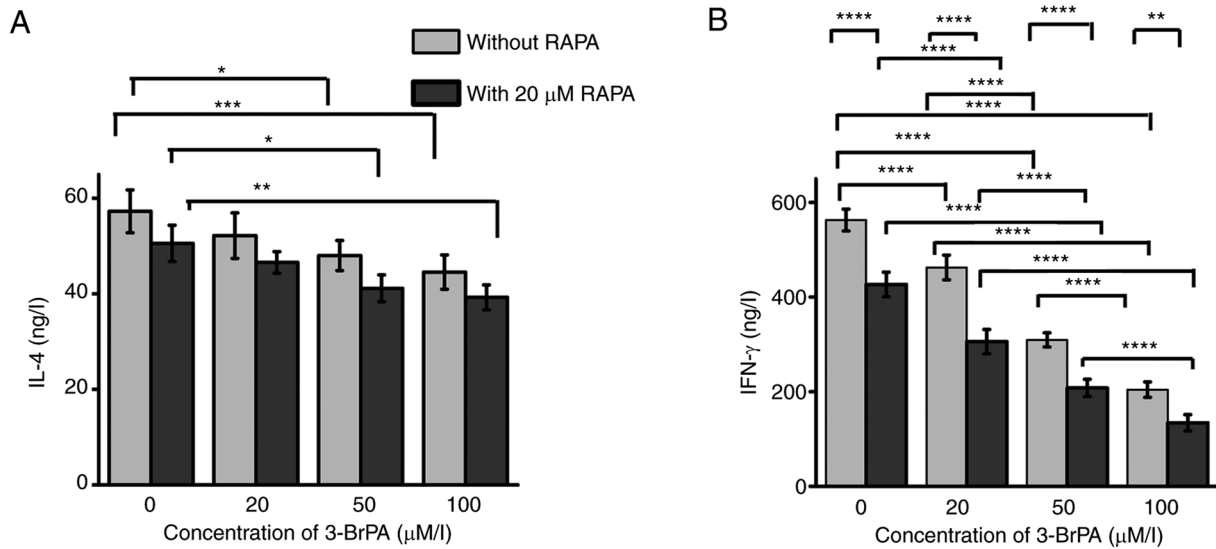


Figure 3. Measurement of IL-4 and IFN- $\gamma$  production after combined treatment with 3-BrPA and RAPA on the MLC for 48 h. (A) IL-4 and (B) IFN- $\gamma$  levels in the media were measured using ELISA. \* $P < 0.05$ , \*\* $P < 0.005$ , \*\*\* $P < 0.001$ , \*\*\*\* $P < 0.0001$ . MLC, mixed lymphocyte culture; RAPA, rapamycin; 3-BrPA, 3-bromopyruvate.

100  $\mu\text{M}$  3-BrPA group (Figs. 2 and S2). Moreover, there were remarkable increase in cellular apoptosis as improving the 3-BrPA concentration from 20 to 100  $\mu\text{M}$  for the combination groups (Figs. 2 and S2).

**IL-4 and IFN- $\gamma$  levels in the MLC.** In terms of IL-4 production, both 3-BrPA treatment alone and combination treatment exerted significant inhibition effects (Fig. 3A). Among the 3-BrPA-alone treatment groups, the 0  $\mu\text{M}$  group showed significantly lower IL-4 production compared to the 50 or 100  $\mu\text{M}$  groups (Fig. 3A). RAPA co-treatment could not mediate a significant difference in IL-4 production compared with that in their corresponding 3-BrPA-alone counterparts at each 3-BrPA concentration tested (Fig. 3A). Among the combined treatment groups, there were significant reduction in IL-4 production comparing the 0  $\mu\text{M}$  3-BrPA group to the 50 or 100  $\mu\text{M}$  3-BrPA groups (Fig. 3A).

Regarding IFN- $\gamma$  production (Fig. 3B), both 3-BrPA alone and combination treatment with RAPA showed significant inhibition effects. There was a cumulative effect between the RAPA and 3-BrPA treatments on the inhibition of IFN- $\gamma$  production. Among the 3-BrPA-alone treatment groups, the IFN- $\gamma$  production decreased when increasing the 3-BrPA concentration (Fig. 3B). Combined treatment alongside RAPA induced significant reductions in IFN- $\gamma$  production compared with that in their corresponding 3-BrPA-alone counterparts at each concentration tested (Fig. 3B). Among the combination treatment groups, the IFN- $\gamma$  production decreased significantly as the concentration of 3-BrPA increased (Fig. 3B).

**Survival time and GVHD score analyses.** Kaplan-Meier survival analysis revealed that all the 3-BrPA- and RAPA-containing treatment groups displayed longer survival time compared with either TBI or aGVHD (Fig. 4A). Additionally, the RAPA plus 3-BrPA and BMT groups demonstrated superior survival compared to the 3-BrPA group, and the BMT group also outperformed the RAPA-2.5 mg group

in terms of survival (Fig. 4A). The combination treatment group showed the highest median survival time among all the treatment groups (Fig. 4B). The RAPA-5 mg group displayed slightly higher median survival time compared with that in the RAPA-2.5 mg group. By contrast, the median survival time in the 3-BrPA group was inferior compared with that in the RAPA-2.5 mg group (Fig. 4B).

The chimeric ratios in the aGVHD, 3-BrPA, 2.5 and 5 mg RAPA groups, the combination treatment group, and BMT group were found to be  $93.1 \pm 2.6$ ,  $95.1 \pm 3.4$ ,  $93.7 \pm 3.8$ ,  $94.2 \pm 3.1$ ,  $95.6 \pm 3.5\%$  and  $95.3 \pm 2.8\%$ , respectively (Fig. S3). There were no significant differences among these groups, suggesting high efficacy of bone marrow transplantation in hemopoietic system regeneration.

Regarding the GVHD scores, it was found that there were significant differences among the groups on days 7, 14 and 21 (Fig. 5). On day 7, there were significant decrease of GVHD score in RAPA-5 mg, RAPA plus 3-BrPA and BMT compared to aGVHD group (Fig. 5). The RAPA plus 3-BrPA and BMT groups also displayed reduced GVHD scores than the 3-BrPA group (Fig. 5). On day 14, 3-BrPA showed significant higher GVHD score than the ones of RAPA-5 mg, RAPA plus 3-BrPA and BMT (Fig. 5). RAPA-2.5 mg also demonstrated superior GVHD score to the RAPA plus 3-BrPA and BMT (Fig. 5). On day 21, RAPA-2.5 mg showed remarkably higher GVHD score than RAPA plus 3-BrPA and BMT (Fig. 5).

**Histological analysis of lung and liver tissues from mice with aGVHD mice.** In the lung tissues (Fig. 6A), those from the 5-mg RAPA treatment group showed reduced levels of small blood clots compared with those in the 3-BrPA and 2.5-mg RAPA treatment groups. The tissues from the combined treatment group only showed capillary dilatation without obvious blood clots (Fig. 6A). In the liver tissues (Fig. 6A), fatty deposits could be observed after 3-BrPA treatment. The 5-mg RAPA treatment group and the combination treatment group presented features that are also comparable to those

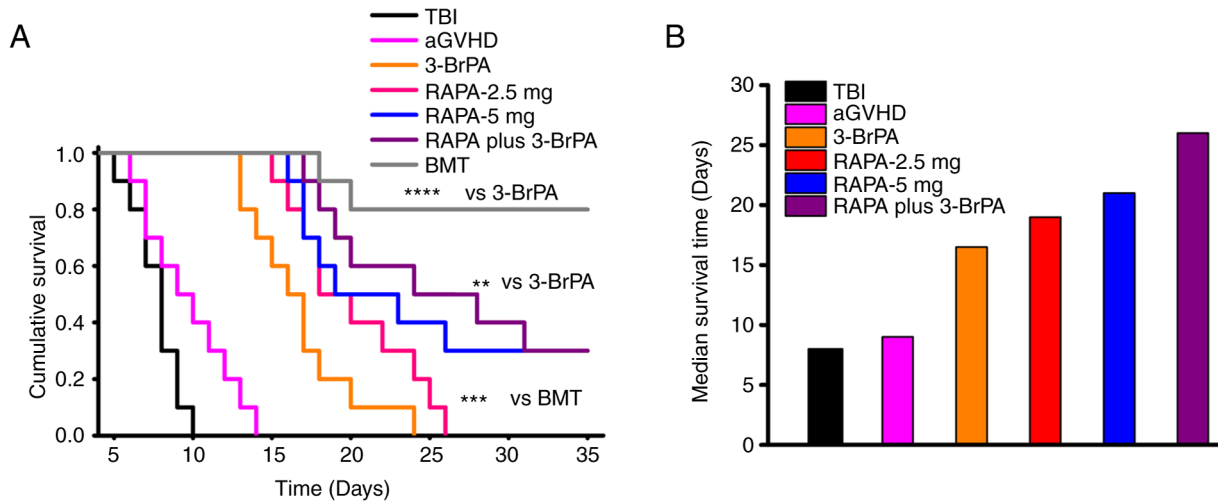


Figure 4. Synergistic effects of RAPA and 3-BrPA on the survival time of mice with aGVHD. (A) Cumulative survival time among the groups as a Kaplan-Meier curve. \*\* $P < 0.005$ , \*\*\* $P < 0.001$ , \*\*\*\* $P < 0.0001$ . (B) Median survival time among the groups. Based on the Bonferroni's correction analysis,  $P < 0.00238$  was considered to indicate a statistically significant difference.  $n = 13$ . aGVHD, acute graft vs. host disease; TBI, total body irradiation; BMT, bone marrow transplantation; RAPA, rapamycin; 3-BrPA, 3-bromopyruvate.

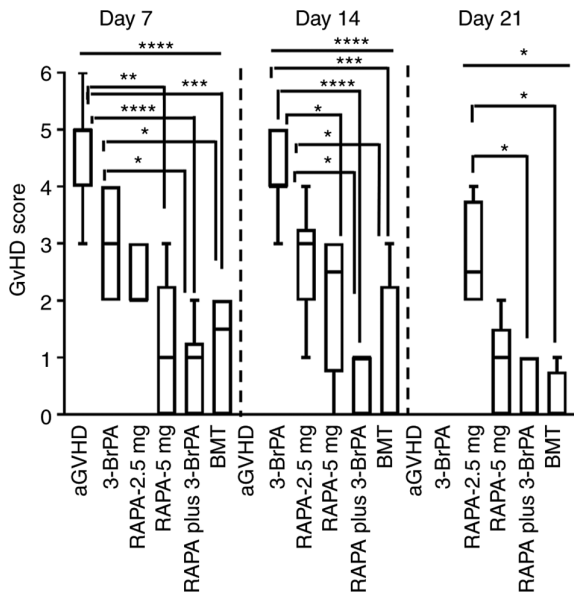


Figure 5. GVHD scores among the groups 7, 14 and 21 days after both bone marrow and spleen cell transplantation. The absences of bars in aGVHD and 3-BrPA groups in Day 14 and Day 21 were due to the death of all mice in these two groups. The mice were treated with 3-BrPA and RAPA daily for 7 days immediately after cell transplantation. \* $P < 0.05$ , \*\* $P < 0.005$ , \*\*\* $P < 0.001$ , \*\*\*\* $P < 0.0001$ . aGVHD, acute graft vs. host disease; TBI, total body irradiation; BMT, bone marrow transplantation; RAPA, rapamycin; 3-BrPA, 3-bromopyruvate.

in the control, without clear signs of inflammation or tissue necrosis.

It was subsequently found that there were significant differences among the groups for the histological scores in the lung and liver tissues (Fig. 6B). For the histological scores in the lung, the Control showed significantly lower histological score than the aGVHD, 3-BrPA or RAPA-2.5 mg groups (Fig. 6B). Treatment with 5 mg RAPA and RAPA plus 3-BrPA resulted in recovery of the lung, as there were no significant differences in the scores compared with those in the control group

(Fig. 6B). In addition, these two treatments induced significant reductions in the histological score compared with those in the aGVHD group (Fig. 6B). RAPA plus 3-BrPA treatment mediated significant reductions in the score compared with that in the 3-BrPA group (Fig. 6B).

For the histological score of the liver, aGVHD and 3-BrPA groups showed higher histological scores than the Control (Fig. 6B). But there were no significant differences between Control and RAPA-2.5 mg, RAPA-5 mg or RAPA plus 3-BrPA, indicating these treatments were efficient in prevention of aGVHD (Fig. 6B). Furthermore, aGVHD showed significant higher histological score than RAPA-5 mg or RAPA plus 3-BrPA, suggesting that these two treatments were viable for alleviating liver damage caused by aGVHD. The RAPA-5 mg group also showed a significant decrease compared with that in the 3-BrPA group (Fig. 6B).

**IL-4 and IFN- $\gamma$  levels in mice with aGVHD.** Regarding *in vivo* IL-4 production (Fig. 7A), there were significant differences among the groups. The Control group showed lower IL-4 production compared to the aGVHD, 3-BrPA, RAPA-2.5 mg and the combination treatment group (Fig. 7A). The TBI group only showed inferior IL-4 production to the aGVHD and 3-BrPA group (Fig. 7A). Additionally, there were no significant differences between aGVHD and 3-BrPA, RAPA-2.5 mg, RAPA-5 mg or RAPA plus 3-BrPA (Fig. 7A). There were also no significant differences among the RAPA-containing treatment groups (Fig. 7A). The 3-BrPA group showed a significantly higher level of IL-4 production compared with that of the RAPA-5 mg group, but without significant differences by comparing to the RAPA-2.5 mg or RAPA plus 3-BrPA group.

In terms of IFN- $\gamma$  (Fig. 7B), there were significant differences among the groups. Control group showed the least IFN- $\gamma$  production among the groups (Fig. 7B). The TBI group showed inferior IFN- $\gamma$  production compared to aGVHD group but superior IFN- $\gamma$  production to the combination treatment group (Fig. 7B). The aGVHD group showed the highest IFN- $\gamma$  production among the groups (Fig. 7B). After 3-BrPA

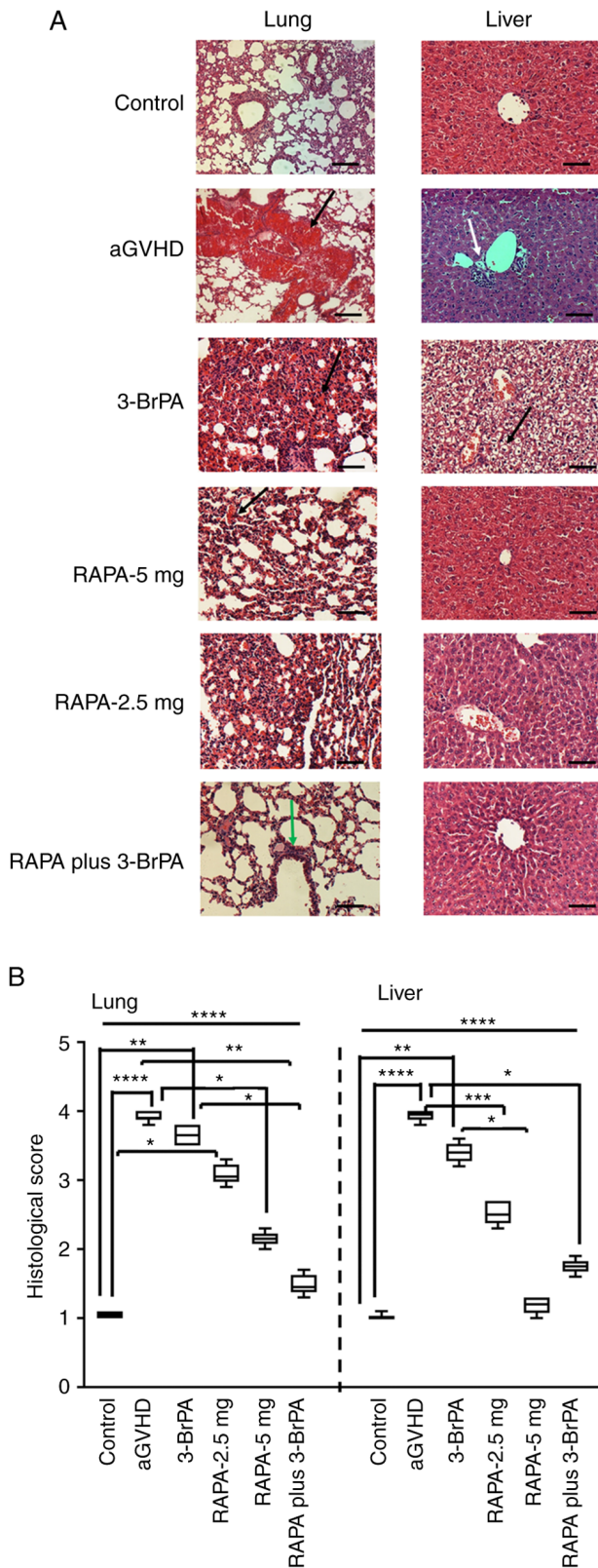


Figure 6. H&E staining and quantitative evaluation of the lung and liver from the mice after transplantation. (A) H&E staining images and (B) corresponding pathological scoring. Black arrows showed the blood clots formed in the lung tissue during aGVHD, the green arrow indicated capillary dilatation. In the right panel of (A), white arrow indicated tissue necrosis and the black arrow indicated the fat granules formed in the liver. Before drug treatment, all mice underwent total body radiation before bone marrow and spleen cell transplantation. \* $P < 0.05$ , \*\* $P < 0.005$ , \*\*\* $P < 0.001$ , \*\*\*\* $P < 0.0001$ . Scale bar, 100  $\mu\text{m}$ . aGVHD, acute graft vs. host disease; TBI, total body irradiation; BMT, bone marrow transplantation; RAPA, rapamycin; 3-BrPA, 3-bromopyruvate.

and/or RAPA treatment, the IFN- $\gamma$  production was significantly reduced compared to the aGVHD group (Fig. 7B). Among the 3-BrPA and/or RAPA treatment groups, the combination treatment group induced the lowest IFN- $\gamma$  level (Fig. 7B). The RAPA-5 mg group showed lower IFN- $\gamma$  production compared with 3-BrPA and RAPA-2.5 mg groups.

## Discussion

To synergistically improve the aGVHD treatment outcome, the glycolysis inhibitor 3-BrPA was combined with the mTOR inhibitor RAPA to target activated T cells in the present study. This strategy revealed desirable synergistic effects in inhibiting the viability of activated T cells. This combined treatment method also potentiated the apoptosis of activated T cells. In addition, decreased production of the proinflammatory cytokine IFN- $\gamma$  validated the potential efficacy of this strategy further. This combination of low-dose RAPA and 3-BrPA treatment also yielded promising outcomes in the *in vivo* aGVHD mouse model by prolonging the survival time. These preclinical results support the hypothesis that 3-BrPA and RAPA can mediate synergistic effects in preventing aGVHD, providing a potentially feasible approach to address this condition.

It has been previously reported that both 3-BrPA and RAPA possess profound anti-cancer properties (27). However, their mechanisms of action are distinct. 3-BrPA exerts its function by targeting GAPDH and hexokinase by alkylating their active sites, with the former serving as the predominant inhibition pathway (17). Additionally, 3-BrPA can also target the HIF-1 $\alpha$  pathway to regulate GAPDH activity further (15,28). It has been reported that administration of 3-BrPA led to the depletion of intracellular ATP in breast cancer cells and thus to deprive cells of energy, inhibiting cell proliferation whilst inducing cytotoxicity and cell apoptosis (15). RAPA is also called Sirolimus and binds to mTOR, which serves key roles in nutrient metabolism regulation, cell proliferation and survival (26). In a previous aGVHD study, RAPA was found to induce the apoptotic cell death of conventional CD4<sup>+</sup>CD25<sup>-</sup> T cells by inhibiting the mTOR/PI3K pathway (29). Another previous study demonstrated the immunosuppressive effects of RAPA on Treg and CD8<sup>+</sup> T cells in mice model (30). In the present study, the combination of 3-BrPA and RAPA were tested on activated T cells before subsequently investigating their effects on an *in vivo* aGVHD model.

In the *in vitro* MLR model, application of 3-BrPA alone significantly inhibited cell viability at doses as low as 20  $\mu\text{M}$ . This is most likely due to the potent inhibition of the glycolytic energy production pathway in the rapidly proliferating and differentiating T cells (18). Additionally, combined treatment exhibited synergism in inhibiting cell viability even when the 3-BrPA concentration was 20  $\mu\text{M}$ . This synergistic effect mediated by low doses of both 3-BrPA and RAPA could be of clinical importance for the treatment of aGVHD, because the application of RAPA is highly compromised by adverse side effects (31).

The reduced cell viability observed in the present study may be caused by the inhibition of cell proliferation or reduction of cell number. Therefore, the extent of T cell apoptosis was next measured. Severe cell apoptosis was observed following

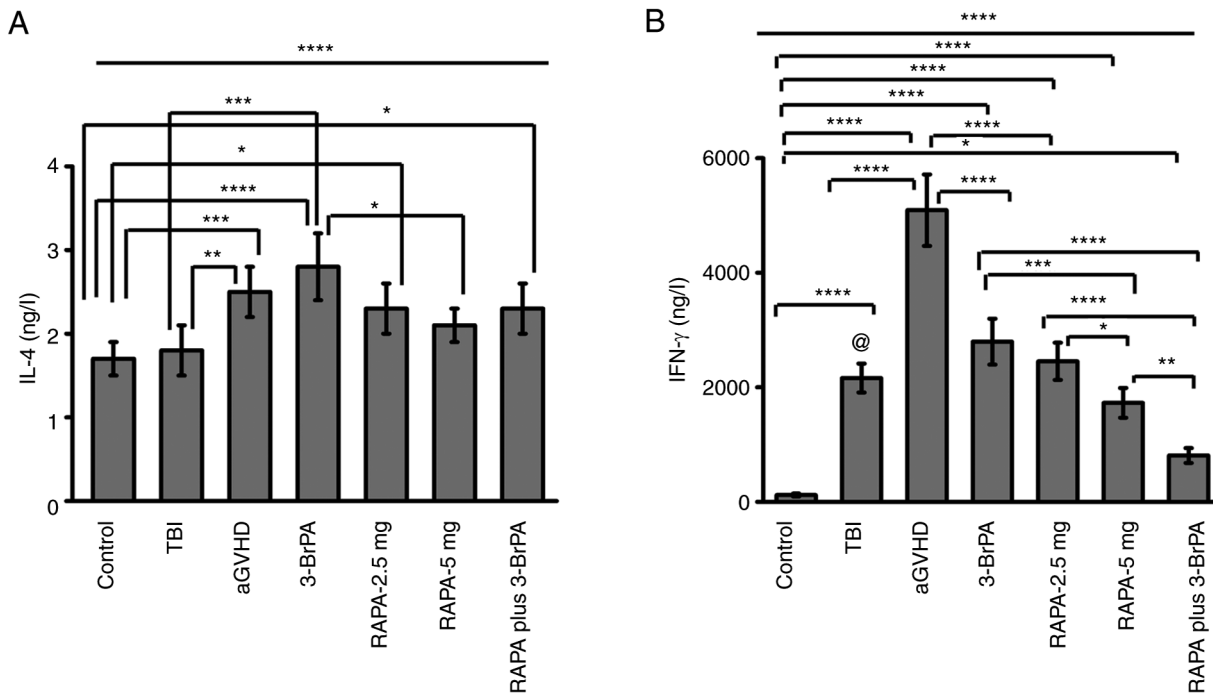


Figure 7. IL-4 and IFN- $\gamma$  levels in the blood of the mice 7 days after bone marrow and spleen cell transplantation and subsequent drug treatments. Mouse blood (A) IL-4 and (B) IFN- $\gamma$  levels were measured using ELISA. \* $P < 0.05$ , \*\* $P < 0.005$ , \*\*\* $P < 0.001$ , \*\*\*\* $P < 0.0001$ . @ $P < 0.0001$  comparing to RAPA plus 3-BrPA groups. aGVHD, acute graft vs. host disease; TBI, total body irradiation; BMT, bone marrow transplantation; RAPA, rapamycin; 3-BrPA, 3-bromopyruvate.

combined drug treatment. This was likely to be due to the vital energy pathways of HIF-1 $\alpha$ , GAPDH and mTOR all being suppressed. Results from the present study are consistent with those from a previous study (18), which reported that RAPA treatment enhanced the anti-tumor capacity of 3-BrPA in lung cancer cell lines H1299 and H23. Treatment with both 3-BrPA and RAPA resulted in the apoptosis of T cells in a synergistic manner. Therefore, this strategy provides a promising option for the prevention of GVHD.

T helper 1 (Th1) and T helper 2 (Th2) CD4<sup>+</sup> T cells can regulate aGVHD by producing a variety of cytokines (32). Th1 cells mainly produce IFN- $\gamma$ , TNF- $\beta$  and IL-2, while Th2 cells mainly secrete IL-4, IL-5, IL-6 and IL-10 (29). Th1 cells are associated with the development of aGVHD, whilst Th2 cells are able to reduce the severity of GVHD (32). Therefore, Th1/Th2 polarization serves a critical role in aGVHD pathogenesis (33), such that targeting Th1 transcription factors can prevent GvHD (34). In the present study, the relatively stable IL-4 levels among the treatment groups but markedly reduced IFN- $\gamma$  levels in the combined treatment groups suggest that the inhibitory effects of this treatment were mainly exerted on Th1 cells instead of Th2 cells. In future studies, the populations of Th1 and Th2 cells after RAPA and 3-BrPA treatment should be investigated.

In the efferent stage of aGVHD, activated T cells and inflammatory cytokines coordinate to attack target tissues and damage the organs (32). These cells include Th1 cells and cytotoxic CD8<sup>+</sup> cells, with cytokines including IFN- $\gamma$  and TNF- $\beta$  (35). In the present aGVHD mouse model, it was found that the administration of 3-BrPA, RAPA and both treatments combined mitigated the damage mediated by aGVHD in the main organs, which was likely to be due to the inhibition of various different pathways in the activated T cells, such as

mTOR and glycolysis. These findings are consistent with a previous study by Nguyen *et al* (8), which found that glycolysis inhibition can ameliorate aGVHD after allo-HSCT in mice. In that previous study, another glycolysis inhibitor 3-(3-pyridinyl)-1-(4-pyridinyl)-2-propen-1-one was applied to inhibit glycolysis, by targeting 6-phosphofructo-2-kinase (8). The staining results in the present study revealed that the combination treatment group appears to be superior compared with the 3-BrPA and low-dose RAPA treatment groups whilst being similar to the 5-mg RAPA treatment group. In the 3-BrPA group, inhibition of glycolysis in the mice also induced lipid deposition in the liver. However, this was not observed in the combined treatment group, likely due to the reduced dose of 3-BrPA.

*In vivo* cytokine levels are important indicators of aGVHD (33). IFN- $\gamma$  levels in the serum has been previously associated with the severity of aGVHD (36). Findings from the present study also support this conclusion, since the aGVHD group presented higher IFN- $\gamma$  levels compared with those in the control. In addition, inhibition of GAPDH, mTOR or both pathways efficiently reduced the IFN- $\gamma$  levels, indicating successful suppression of the activity of Th1 cells. Since there were no obvious changes in the IL-4 levels after any of the treatments, the direction of Th1/Th2 polarization was likely to be biased towards the Th2 subset. Although it would be of interest to perform western blotting assay to evaluate the key targets of both mTOR and glycolytic pathways, it was not possible to obtain the required volume of blood from each mouse for the isolation of sufficient T cells for western blotting. Therefore, only the cytokine concentration from the blood was measured using ELISA in the present study.

Minimizing GVHD whilst maximizing the GvT effect is the ideal outcome of HSCT (20). There is a limitation in the

present study, only the prevention of aGVHD by combining the glycolysis inhibitor 3-BrPA and the mTOR inhibitor RAPA was focused upon. In future experiments, the GvT effect of this combination treatment can be evaluated on animals with blood cancer (such as leukemia, lymphoma and myeloma) and underwent HSCT. This combination is advantageous, since both the *in vitro* and *in vivo* data confirmed the high efficacy of this strategy. Furthermore, this approach likely exerts synergistic GvT effects, since the glycolysis inhibitor is able to suppress cancer cell viability whereas mTOR inhibition can hinder the proliferation and survival of cancer cells. In future studies, the influence of this system on the GvT effect, in addition to other immune cell types, such as Tregs and MDSCs (20), should be studied.

In conclusion, the present study applied both *in vitro* MLR and *in vivo* aGVHD mouse models to reveal that glycolysis inhibition is an efficient approach for aGVHD prevention. Furthermore, combination treatment with 3-BrPA plus low-dose RAPA appears to be advantageous, since it targets multiple signaling pathways and requires lower doses of RAPA. Therefore, the present study opened a novel avenue for aGVHD prevention and treatment. In the future, introducing novel glycolysis inhibitors and immunosuppressors with minimal side effects and higher efficacy to target multiple signaling pathways would be highly desirable for the combination therapy of aGVHD.

#### Acknowledgements

Not applicable.

#### Funding

The present study was supported by the Natural Science Foundation of China (grant no. 81600147), the Zhongshan Science and Technology Research Major Project (grant no. 2017B002), Shenzhen Science and Technology Plan Basic Research Project (grant nos. JCYJ20180307150408596 and JCYJ20190809172403604), Sanming Project of Medicine in Shenzhen (grant no. SZSM201911004), the Fundamental Research Funds for the Central (grant no. 2175060), Starting Grant from The Seventh Affiliated Hospital Sun Yat-sen University (grant no. ZSQYRSF0008) and The Young Talents Fostering Grant from Sun Yat-sen University (grant no. 20ykpy18).

#### Availability of data and materials

The datasets used and/or analyzed during the current study are available from the corresponding author on reasonable request.

#### Authors' contributions

RQZ and XJX confirm the authenticity of all the raw data. RQZ analyzed and interpreted data and wrote the manuscript. XBW and YBY analyzed and interpreted data. BL analyzed *in vitro* data. JW, ZWG and PS analyzed *in vitro* data. WJM and ZY analyzed *in vivo* data. LPY supervised the study, analyzed and interpreted data and wrote and edited the manuscript. XJX

conceived and designed the study and revised the manuscript. All authors have read and approved the final manuscript.

#### Ethics approval and consent to participate

All animal experiments were approved by the Ethics Committee of Southern Medical University (Guangzhou, China) and fulfilled the regulations of Institutional Animal Care and Use Committee.

#### Patient consent for publication

Not applicable.

#### Competing interests

The authors declare that they have no competing interests.

#### References

1. Singh AK and McGuirk JP: Allogeneic stem cell transplantation: A historical and scientific overview. *Cancer Res* 76: 6445-6451, 2016.
2. de Witte T, Bowen D, Robin M, Malcovati L, Niederwieser D, Yakoub-Agha I, Mufti GJ, Fenaux P, Sanz G, Martino R, *et al*: Allogeneic hematopoietic stem cell transplantation for MDS and CMML: Recommendations from an international expert panel. *Blood* 129: 1753-1762, 2017.
3. Schmitz N, Lenz G and Stelljes M: Allogeneic hematopoietic stem cell transplantation for T-cell lymphomas. *Blood* 132: 245-253, 2018.
4. Gonsalves WI, Buadi FK, Ailawadhi S, Bergsagel PL, Khan AA, Dingli D, Dispenzieri A, Fonseca R, Hayman SR, Kapoor P, *et al*: Utilization of hematopoietic stem cell transplantation for the treatment of multiple myeloma: A mayo stratification of myeloma and risk-adapted therapy (mSMART) consensus statement. *Bone Marrow Transplant* 54: 353-367, 2019.
5. Ghimire S, Weber D, Mavin E, Wang XN, Dickinson AM and Holler E: Pathophysiology of GvHD and other HSCT-related major complications. *Front Immunol* 8: 79, 2017.
6. Bhatia S, Armenian SH and Landier W: How I monitor long-term and late effects after blood or marrow transplantation. *Blood* 130: 1302-1314, 2017.
7. Zeiser R and Blazar BR: Acute graft-versus-host disease-biologic process, prevention, and therapy. *N Eng J Med* 377: 2167-2179, 2017.
8. Nguyen HD, Chatterjee S, Haarberg KM, Wu Y, Bastian D, Heinrichs J, Fu J, Daenthanasannak A, Schutt S, Shrestha S, *et al*: Metabolic reprogramming of alloantigen-activated T cells after hematopoietic cell transplantation. *J Clin Invest* 126: 1337-1352, 2016.
9. Pearce EL, Poffenberger MC, Chang CH and Jones RG: Fueling immunity: Insights into metabolism and lymphocyte function. *Science* 342: 1242-1245, 2013.
10. Gatza E, Wahl DR, Opipari AW, Sundberg TB, Reddy P, Liu C, Glick GD and Ferrara JLM: Manipulating the bioenergetics of alloreactive T cells causes their selective apoptosis and arrests graft-versus-host disease. *Sci Transl Med* 3: 67ra8, 2011.
11. Byersdorfer CA, Tkachev V, Opipari AW, Goodell S, Swanson J, Sandquist S, Glick GD and Ferrara JLM: Effector T cells require fatty acid metabolism during murine graft-versus-host disease. *Blood* 122: 3230-3237, 2013.
12. Akers LJ, Fang W, Levy AG, Franklin AR, Huang P and Zweidler-McKay PA: Targeting glycolysis in leukemia: A novel inhibitor 3-BrOP in combination with rapamycin. *Leuk Res* 35: 814-820, 2011.
13. Xu RH, Pelicano H, Zhang H, Giles FJ, Keating MJ and Huang P: Synergistic effect of targeting mTOR by rapamycin and depleting ATP by inhibition of glycolysis in lymphoma and leukemia cells. *Leukemia* 19: 2153-2158, 2005.
14. Zhou S, Min Z, Sun K, Qu S, Zhou J, Duan H, Liu H, Liu X, Gong Z and Li D: MiR-199a-3p/Sp1/LDHA axis controls aerobic glycolysis in testicular tumor cells. *Int J Mol Med* 42: 2163-2174, 2018.

15. Attia YM, El-Abhar HS, Al Marzabani MM and Shouman SA: Targeting glycolysis by 3-bromopyruvate improves tamoxifen cytotoxicity of breast cancer cell lines. *BMC Cancer* 15: 838, 2015.
16. Del Rey MJ, Valín A, Usategui A, García-Herrero CM, Sánchez-Aragó M, Cuezva JM, Galindo M, Bravo B, Cañete JD, Blanco FJ, *et al*: Hif-1 $\alpha$  knockdown reduces glycolytic metabolism and induces cell death of human synovial fibroblasts under normoxic conditions. *Sci Rep* 7: 3644, 2017.
17. Abdel-Wahab AF, Mahmoud W and Al-Harizy RM: Targeting glucose metabolism to suppress cancer progression: Prospective of anti-glycolytic cancer therapy. *Pharmacol Res* 150: 104511, 2019.
18. Zhang Q, Pan J, Lubet RA, Komar SM, Kalyanaraman B, Wang Y and You M: Enhanced antitumor activity of 3-bromopyruvate in combination with rapamycin in vivo and in vitro. *Cancer Prev Res (Phila)* 8: 318-326, 2015.
19. Palmer JM, Chen BJ, DeOliveira D, Le ND and Chao NJ: Novel mechanism of rapamycin in GVHD: Increase in interstitial regulatory T cells. *Bone Marrow Transplant* 45: 379-384, 2010.
20. Scheurer J, Reisser T, Leithäuser F, Messmann JJ, Holzmann K, Debatin KM and Strauss G: Rapamycin-based graft-versus-host disease prophylaxis increases the immunosuppressivity of myeloid-derived suppressor cells without affecting T cells and anti-tumor cytotoxicity. *Clin Exp Immunol* 202: 407-422, 2020.
21. Gruppuso PA, Boylan JM and Sanders JA: The physiology and pathophysiology of rapamycin resistance: Implications for cancer. *Cell Cycle* 10: 1050-1058, 2011.
22. Fantini MC, Dominitzki S, Rizzo A, Neurath MF and Becker C: In vitro generation of CD4<sup>+</sup> CD25<sup>+</sup> regulatory cells from murine naive T cells. *Nat Protoc* 2: 1789-1794, 2007.
23. Chou TC: Drug combination studies and their synergy quantification using the chou-talalay method. *Cancer Res* 70: 440-446, 2010.
24. Ni X, Xia Y, Zhou S, Peng H, Wu X, Lu H, Wang H, Liu R, Blazar BR, Gu J and Lu L: Reduction in murine acute GVHD severity by human gingival tissue-derived mesenchymal stem cells via the CD39 pathways. *Cell Death Dis* 10: 13, 2019.
25. Liu Q, Ning J, Zhang Y, Wu X, Luo X and Fan Z: Idiopathic pneumonia syndrome in mice after allogeneic bone marrow transplantation: Association between idiopathic pneumonia syndrome and acute graft-versus-host disease. *Transpl Immunol* 23: 12-17, 2010.
26. Cooke KR, Kobzik L, Martin TR, Brewer J, Delmonte J Jr, Crawford JM and Ferrara JL: An experimental model of idiopathic pneumonia syndrome after bone marrow transplantation: I. The roles of minor H antigens and endotoxin. *Blood* 88: 3230-3239, 1996.
27. Ju XP, Xu B, Xiao ZP, Li JY, Chen L, Lu SQ and Huang ZX: Cytokine expression during acute graft-versus-host disease after allogeneic peripheral stem cell transplantation. *Bone Marrow Transplant* 35: 1179-1186, 2005.
28. Shi LZ, Wang R, Huang G, Vogel P, Neale G, Green DR and Chi H: HIF1 $\alpha$ -dependent glycolytic pathway orchestrates a metabolic checkpoint for the differentiation of TH17 and Treg cells. *J Exp Med* 208: 1367-1376, 2011.
29. Shin HJ, Baker J, Leveson-Gower DB, Smith AT, Sega EI and Negrin RS: Rapamycin and IL-2 reduce lethal acute graft-versus-host disease associated with increased expansion of donor type CD4<sup>+</sup>CD25<sup>+</sup>Foxp3<sup>+</sup> regulatory T cells. *Blood* 118: 2342-2350, 2011.
30. Zeiser R, Nguyen VH, Beilhack A, Buess M, Schulz S, Baker J, Contag CH and Negrin RS: Inhibition of CD4<sup>+</sup>CD25<sup>+</sup> regulatory T-cell function by calcineurin-dependent interleukin-2 production. *Blood* 108: 390-399, 2006.
31. Sánchez-Fructuoso AI, Ruiz JC, Pérez-Flores I, Alamillo CG, Romero NC and Arias M: Comparative analysis of adverse events requiring suspension of mTOR inhibitors: Everolimus versus sirolimus. *Transplant Proc* 42: 3050-3052, 2010.
32. Nikolic B, Lee S, Bronson RT, Grusby MJ and Sykes M: Th1 and Th2 mediate acute graft-versus-host disease, each with distinct end-organ targets. *J Clin Invest* 105: 1289-1298, 2000.
33. Guo H, Qiao Z, Zhu L, Wang H, Su L, Lu Y, Cui Y, Jiang B, Zhu Q and Xu L: Th1/Th2 cytokine profiles and their relationship to clinical features in patients following nonmyeloablative allogeneic stem cell transplantation. *Am J Hematol* 75: 78-83, 2004.
34. Yu Y, Wang D, Liu C, Kaosaard K, Semple K, Anasetti C and Yu XZ: Prevention of GVHD while sparing GVL effect by targeting Th1 and Th17 transcription factor T-bet and ROR $\gamma$ t in mice. *Blood* 118: 5011-5020, 2011.
35. Golubovskaya V and Wu L: Different subsets of T cells, memory, effector functions, and CAR-T immunotherapy. *Cancers (Basel)* 8: 36, 2016.
36. Choi J, Ziga ED, Ritchey J, Collins L, Prior JL, Cooper ML, Piwnica-Worms D and DiPersio JF: IFN $\gamma$ R signaling mediates alloreactive T-cell trafficking and GVHD. *Blood* 120: 4093-4103, 2012.



This work is licensed under a Creative Commons Attribution-NonCommercial-NoDerivatives 4.0 International (CC BY-NC-ND 4.0) License.